Proceedings of 2004 IEEE/RSJ International Conference on
Intelligent Robots and Systems
September 28 - October 2, 2004, Sendai, Japan

Angular Momentum Primitives for Human Walking: Biomechanics and Control

Marko Popovic,
The Media Laboratory
Computer Science and Artificial Intelligence Laboratory
MIT
Cambridge, Massachusetts, USA
marko@media.mit.edu

Amy Englehart
The Media Laboratory
MIT
Cambridge, Massachusetts, USA
amyjoie@media.mit.edu

Hugh Herr
The Media Laboratory
MIT-Harvard Division of Health Sciences & Technology
MIT
Cambridge, Massachusetts, USA
hherr@media.mit.edu

Abstract— **Towards the goal of developing stable humanoid robots and leg prostheses, we present a biologically motivated control strategy for walking where system angular momentum is explicitly controlled. Using human kinematic gait data, we calculate the distribution of spin angular momentum throughout the human body at slow and self-selected walking speeds. Principal Component Analysis reveals three angular momentum primitives that explain 99% of the walking data for sagittal plane body rotations. In addition, our analysis shows that the angular momentum primitives are invariant with walking speed. Using these biomechanical results, we simulate human walking during the single support phase using a morphologically realistic humanoid model walking in the sagittal plane. There is minimal predefined specification of the desired gait motion. With only the model's walking speed and stride length as an input, our control system searches for joint reference trajectories that minimize the error between the model's angular momentum distribution and the biologically determined distribution. Resulting model joint kinematics are in qualitative agreement with human gait data, suggesting that exploiting invariant angular momentum primitives in humanoid control may prove critical to achieving biological realism in legged robots and prostheses. The angular momentum primitives framework can substantially simplify the process of gait synthesis and enable the operator of a humanoid robot or powered leg prosthesis to easily change stride length and/or walking speed.**

Keywords-walking;control; angular momentum

I. INTRODUCTION

Often the central problem with controlling a multi-joint robot interacting with the external world is split into two distinct but coupled problems:

- planning the predefined joint trajectories
- tracking the actualized predefined joint trajectories.

In recent decades successful effort has been devoted to address the latter problem [1]. However, in the field of humanoid robotics, many issues are still left unresolved for the former problem [2].

The ambitious goal of the field of humanoid robotics is to have robots that can perform biomimetic motions and hopefully someday even exceed human capabilities, and dynamical actions in realistic conditions [3-7]. The planning of predefined trajectories for humanoid robots should address the following:

- The joint motions are physically realizable (e.g. the resulting ground reaction force is pointing up and center of pressure (CP) is inside the foot support polygon)[1].
- The required dynamical action is constrained to be within the limits of the plant capabilities.
- The trajectory is optimized such that a large range of disturbances can be rejected.
- Fast transitions from one task's condition to another such as changing the walking speed or to a complete task change such as from walking to running.

[1] As discussed in [8] the CP trajectory can be obtained from the planned joint trajectories. If computed CP falls outside the foot support polygon that should not be necessarily viewed as an indication of postural instability, but rather, as an indication that the planned joint trajectories are not physical. Similarly, the FRI point [9] being outside the foot support polygon should not be always viewed as an indication of postural instability.

0-7803-8463-6/04/$20.00 ©2004 IEEE

- Various metrics of motion quality are optimized as well (e.g. energy expenditure for walking [10] or total torque about plant's center of mass (CM) and sum of joint torques squared [11]).
- Superposition of several tasks (e.g. walking and holding a glass of water).
- Necessary time delays from robot response times.

The realistic humanoid model has more than 30 degrees of freedom (DOF) specifying its movement. As well, various tasks, different conditions for the same task, external world conditions and all their possible combinations are quite numerous. Therefore, it is not just that the optimization problem of finding the best trajectory for one specific activity is very complex but the whole space of possible motion requires immense amounts of memory to contain all the solutions. The natural question then is how is this performed in humans?

We believe that part of the answer is that the predefined trajectories should not be given as very detailed and very precise information and that it should be up to the control algorithm, that operates on a time scale of 100 ms, to decide on all joint trajectories based on high level requirements. In extreme cases, for example for walking task, one could imagine that the predefined trajectory is given only by the simple desired CM trajectory specifications, similar to [11,12,13] and maybe in addition some predefined whole plant angular momentum, similar as proposed in [11,14,15]. The controller, based on the plant's state, then needs to quickly decide on all joint accelerations such that some of the basic balance requirements are satisfied. This concept clearly puts some burden on the controller that needs to perform some type of optimization in real time (i.e. not just a simple PD control about the predefined joint trajectories). With many degrees of freedom and various potential disturbances, the question is how this optimization can be performed rapidly and efficiently.

To deal with the complexity of humanoid movements a reduced order architecture is needed. Recently, the concept of motor primitives has been discussed in the literature in the context of dimensional reduction. Experiments involving multiple point stimulation of a frog's spinal cord [16] demonstrated that a limb's endpoint generated force field obeys the principle of superposition. Moreover, only a small set of primitive force fields was sufficient to explain a large data sample [16]. These findings support hypothesis that the central nervous system may generate a wide repertoire of motor behaviors through the vectorial superposition of a few motor primitives stored within the neural circuits in the spinal cord. Experiments on human reaching movements [17] gave further support for this concept. Theoretical studies [18] correlated system's ability to learn with the actual functional form of its dynamic primitives. The kinematics trajectories of planar human arm were studied [19] and motor movement primitives were obtained based on the principal component decomposition. A similar method has been used for humanoid 3D upper body controllers [20]. The motion primitives were first extracted and then used for control with small set of basic controllers [20].

In this study, the motor primitives approach is used for the first time to analyze whole body movements. Moreover, this is the first study where body segments' spin angular momentum distribution is used to generate motor primitives. Motivation for this approach came from the evidence that for a large class of activities, such as balancing while standing, walking and running, the human body closely regulates total spin angular momentum [11, 21-24].

In this investigation we use principal component analysis to obtain spin angular momentum primitives. We hypothesize that only a small number of primitives are sufficient to explain 95% of the whole body walking data across a range of walking speeds. We further hypothesize that these angular momentum primitives can be used to generate biologically realistic motions in a morphologically realistic human model. Moreover, we anticipate that this approach will simplify the control problem by reducing the whole body state to a much lower dimensional representation. We test these ideas by observing and analyzing biological gait data for one test subject (Section II) and by simulating a single support phase in walking of a 2-D morphologically realistic human model using a control methodology based on angular momentum primitives (Section III). In addition we discuss alternatives to our controller that should increase the robustness of the presented method (Section IV).

II. Biomechanics

A. *Methods: Kinematic Gait Analysis*

Ground reaction forces, center of pressure (CP) trajectory and kinematic data describing human limbs during walking were obtained in the Gait Laboratory of Spaulding Rehabilitation Hospital, Harvard Medical School. The healthy normal subject walked at slow and self-selected moderate speeds for seven trials each. The ground reaction forces were measured using 2 AMTI forceplates (model OR6-5-1, AMTI, Newton, MA) at the frequency of 1080 Hz. The forceplates had a precision of approximately 0.1 Newton. The limb trajectories were acquired using an infrared VICON Motion Capture system (VICON 512, Oxford Metrics, Oxford, England). Thirty-three markers were placed on the subject's body: sixteen lower body markers, five trunk markers, eight upper limb markers and four head markers. Motion data were gathered at a frequency of 120 Hz. Depending on the position and movements of the subject, the VMC could detect the marker positions with a precision of a few millimeters.

The human model [11] used for gait analysis consisted of 16 links: right and left feet, shanks, thighs, hands, forearms, upper arms, the pelvis-abdomen region, the thorax, the neck and the head. The feet and hands were modeled as rectangular boxes. The shanks, thighs, forearms and upper arms were modeled as truncated cones. The pelvis-abdomen link and the thoracic link were modeled as elliptical slabs. The neck was modeled as a cylinder and the head was modeled as a sphere. This model is shown in Fig.

1. About twenty physical measurements of the subject's links dimensions were taken to accurately model the subject. Based on the links' dimensions the link's masses and densities were modeled to closely match the experimental values [25,26]. The human model had a total of 38 degrees of freedom; 32 internal degrees of freedom (12 for the legs, 14 for the arms and 6 for the rest) and 6 external degrees of freedom.

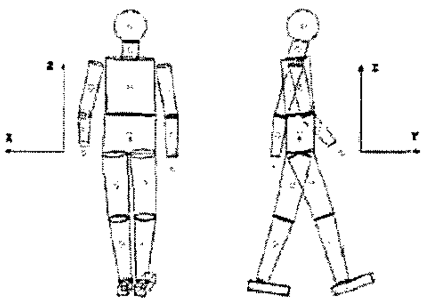

Figure 1. A human model, consisting of 16 rigid links, was used to calculate the distribution of the angular momentum throughout the human body from the gait data.

The angular momentum about the body's CM of each link was calculated as a sum of the orbital and spin components. The orbital component was given as the angular momentum in the body's CM frame of the point mass located at the link's CM with the mass equal to that of the link. The spin component was the angular momentum of the link in the link's CM frame.

Principal component analysis (PCA) was performed on each links' angular momentum, for each of the three spatial components, to give the angular momentum primitives. The eigenvalue problem of the 16 by 16 (16 was the number of links of our human model) data covariance matrix was solved. The eigenvectors were then ordered by the respective size of their eigenvalues. In this way a new 16-dimensional basis was obtained where basis vectors, $\vec{P}_i$, were linearly independent and ordered by their statistical, i.e. data dependent, significance. In principle, only some basis vectors were utilized to reproduce the initial data set at chosen level of precision.

The actual time dependent normalized distribution, $c_i(t)$ of each PC vector $\vec{P}_i$ as a function of the gait cycle was then obtained by the projection method. The projection method finds the scalar product of the ith PC, $\vec{P}_i$, and the normalized gait spin distribution $\vec{L}(t)/|\vec{L}(t)|$ with both represented in the original links' angular momentum basis. The time dependent normalized distribution coefficients satisfy

$$\sum_{i=1}^{16} c_i^2(t) = 1. \qquad (1)$$

B. *Results: Angular momentum primitives*

The first principal components, i.e. angular momentum primitives, in the sagittal, coronal and transverse planes explained approximately 90%, 75% and 85% of the data, respectively. The first three primitives in each plane combined explained 99%, 95%, and 95% of the data, respectively. To compare the PCs of two different speeds their scalar product was found. The scalar product of the first primitives, of the same subject, at slow and moderate walking speeds was larger than 0.99 for all three spatial directions. The scalar product of the second primitives at these same walking speeds was only slightly smaller, or 0.99, 0.98, and 0.97 for sagittal, coronal and transverse plane rotations, respectively. These observations suggest that the angular momentum primitives are largely invariant to walking speed.

Fig. 2 shows the first three angular momentum primitives, with largest data explained. Fig. 3 shows their average normalized distributions, $c_1(t)$, $c_2(t)$ and $c_3(t)$ as a function of the percentage of the gait cycle. In addition to these findings we have also observed that the first three primitives' distributions for slow speed, $c_i^{sl}(t)$, and moderate speed, $c_i^{mo}(t)$, of the same subject overlap at one standard deviation throughout the whole gait cycle with standard deviations on the order of several percent from the mean value. The speed invariance of the PC and their gait cycle dependent normalized distributions makes angular momentum primitives a useful tool for gait synthesis.

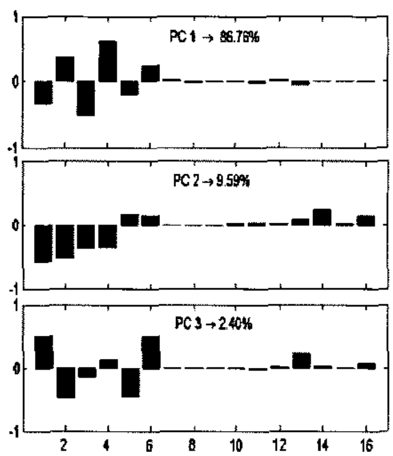

Figure 2. The first three angular momentum primitives in the sagittal plane and their respective data explained. The abscissa numbers and human model links are paired in the following order: left foot (1), right foot (2), left shin (3), right shin (4), left thigh (5), right thigh (6), left hand (7), right hand (8), left forearm (9), right forearm (10), left upper arm (11), right upper arm (12), abdomen and pelvis (13), thorax (14), neck (15) and head (16).

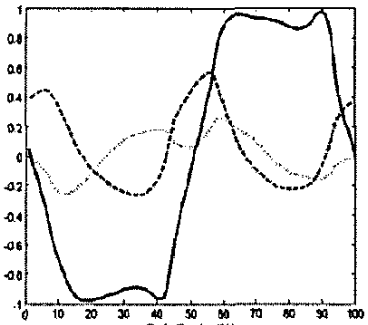

Figure 3. The average distribution of the first three angular momentum primitives as a function of the percentage of the gait cycle. By convention, 0% and 100% represent consecutive heel strikes of the same foot. The first primitive with largest data explained is represented with solid line, the second primitive with a dashed line and the third primitive with a dotted line.

III. Control

A. Methods: Angular momentum primitives

Towards the final goal of developing a biomimetic walking robot, the angular momentum primitives were used to define the motion of a humanoid model following a simple predefined CM trajectory of constant height and speed. Our control system searched for joint reference trajectories that minimized the error between the model's angular momentum distribution and the biologically determined distribution.

As utilized for this controller, given the stride length and walking speed the position in the human gait cycle can be very precisely determined based only on the CM position in respect to the stance foot. This is because the CM deviates only slightly around the point that is moving with constant forward speed. After the estimate on position in the gait cycle was made, the results presented in Fig. 2 and Fig. 3 were used to determine desired biomimetic spin distribution.

B. Methods: Humanoid structural model

The eight degree of freedom (DOF) humanoid model consisted of eight rigid links or appendages: a pair of feet, a pair of shanks, a pair of thighs, a pelvis and abdomen as one link and a thorax. The model moved in the sagittal plane only and had one non-rotating stance foot at all time. This gave the model effectively seven DOF.

C. Methods: Control algorithm

Fig. 4 illustrates the control method employed for our current simulation and results. For this implementation, the Robot block and the Dynamics Model block were equivalent. The general flow of the controller is described below. Based on the robot's actual joint angles, $\vec{q}(t)$, joint angular velocities, $\vec{q}^{\,'}(t)$ and joint angular accelerations, $\vec{q}^{\,''}(t)$, an initial optimizer quickly determined a suggestion for the next time step's joint accelerations based on the spin distribution data. The final optimizer then finely tuned the offered solution by performing a more sophisticated search in the close vicinity of the initial optimizer's suggested joint acceleration vector for the next time step's joint accelerations. The optimization was based on minimizing the cost function from the vector of terms, $\vec{y}(t)$. These fully-optimized joint accelerations were applied to the robot. The robot's actual kinetic data then updated the cost function and simultaneously began the initial optimizer for the next time step.

The concept behind the initial optimizer is as follows. Given the estimated CM position and velocity at the next time step together with the stance foot position, the spin of the stance foot at the next time step was calculated. The controller then estimated the appropriate gait phase and used the speed invariant biological spin distribution to generate the links' desired angular momentum at the next time step. Given this desired angular momentum distribution, the joints' desired angular accelerations were determined. This solution then served as the initial guess for the final optimizer.

The procedure to generate the links' desired angular momentum consisted of optimizing the stance ankle acceleration so that the shin's angular momentum matches the desired spin. The same procedure is then applied to the knee joint, so that the stance thigh's angular momentum matched the desired one, and this was continued for all other joints. By starting with known foot dynamics the whole body spin distribution was optimized to reproduce the biological distribution. This procedure significantly simplified the process of spin distribution optimization. Instead of a complex nonlinear optimization problem defined in N-dimensional space, where N is the number of degrees of freedom, the problem is reduced to N simpler one-dimensional problems. With a 2.4 GHz PC used for our simulations, the time for obtaining the initial optimizer's solution was generally two orders of magnitude smaller than the size of the physical time step, 0.25 ms.

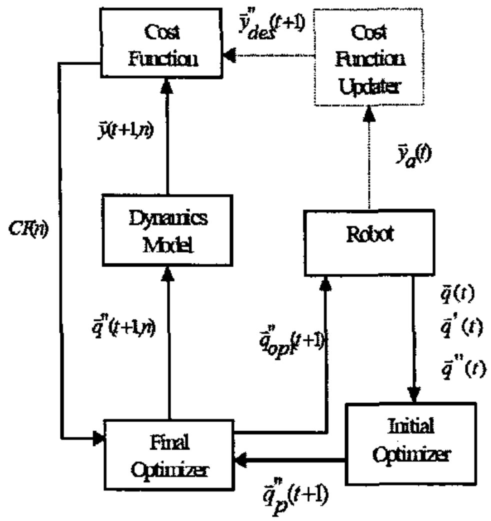

Figure 4. Block diagram of controller. The vectors $\vec{q}(t)$, $\vec{q}\,'(t)$ and $\vec{q}\,''(t)$ denote the position, velocity and acceleration of the robot's joints. The vector $\vec{y}(t)$ denotes the cost function terms to be optimized. The subscript's a and p denote, respectively the actual robot values and the best guess for the next joint accelerations based on the initial optimizer. The subscript n denotes the nth iteration of the optimizer. The variable $CF(n)$ is the cost of the nth iteration of joint accelerations. The subscript des denotes the suggested change to the cost function terms based on the robot's actual response. The subscript opt denotes the lowest cost choice of new joint accelerations.

The effect of numerical errors in the estimated CM position and velocity, and errors in the appropriate gait phase estimates, was compounded for links that were further apart from the stance leg foot. In the current implementation, to increase the quality of the initial optimizer's solution, the swing leg's hip, knee and ankle joint angular accelerations were also optimized to secure foot clearance, to minimize the error between the actual and desired CM trajectory and each joint's acceleration was constrained so that the joint's angles at the next simulation step were inside the biological angle ranges. In addition, the swing leg motion was optimized to ensure that the vertical projection of the CM onto the ground was close to the center of the projected-swing-foot support polygon (PSP).

The PSP was defined here as the polygon that encloses the stance foot and the vertical projection of the swing foot onto the ground. In gait studies we observed that the projected CM position always falls inside the PSP and is never too far from its center. This may represent part of the human motor control strategy for addressing small to medium size disturbances. When efforts to balance cause the swing leg to suddenly step down, it is likely to be beneficial that the CM projection is not very far from the center of the PSP so that the plant could be most efficiently stabilized.

When the starting guess was specified, the final optimizer performed a medium-local gradient based type of search in the large N dimensional space with small, limited number of search points. With a Matlab based (Mathworks, Natick, MA) implementation and several hundred search points this optimization took about 80 ms real processing time for the simulation's 25 ms time increment. The cost function included the sum of biologically weighted joint torques squared, where weighting factors are given by the biological peak values for the single support, the sum of joint torque derivatives squared and the desired CM position and CM velocity. The desired CM trajectory was represented as a point moving with constant speed. The cost function included very large terms to limit joint angles to biological ranges, and moderate terms to match biological spin distribution. The cost function included a term that penalized the FRI point proximity to the edge of the foot support polygon depending on the gait phase and a term that ensured the foot clearance also depending on the gait phase.

To test the appropriateness of the gradient based search performed by the final optimizer we experimented with another version of the final optimizer using the same cost function and utilizing a genetic algorithm type of search in a much larger volume of the N-dimensional space. In this case, for about 10^6 search steps, the final optimizer's search took an order of 100 s per simulation's 25 ms time increment.

D. *Control: Results*

Fig. 5 shows six consecutive poses of the two-dimensional toy sagittal human model for the single support phase using the local gradient based final optimizer. The target CM, emergent CM, emergent FRI point together with emergent ground reaction force vector are also shown. This dynamical motion was obtained using the controller with a specified initial condition obtained from the biological gait data. Fig. 6 shows the joint angles (hip, knee and ankle for stance and swing leg) together with the actual biological gait data for comparison.

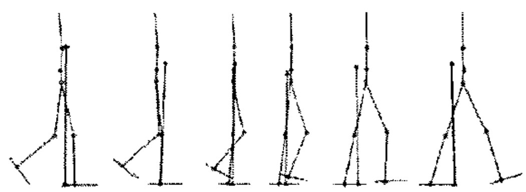

Figure 5. Six consecutive poses from the simulation of the sagittal model in the single support phase. The target CM is represented with a cross and the actual simulation's CM is denoted with a diamond. The ground reaction force vector is represented with an arrow and it originates at the FRI point moving beneath the stance foot. The force magnitude is represented so that 1 N corresponds to 2 mm of the actual humanoid model's dimensions. Height of the CM is approximately 1 m.

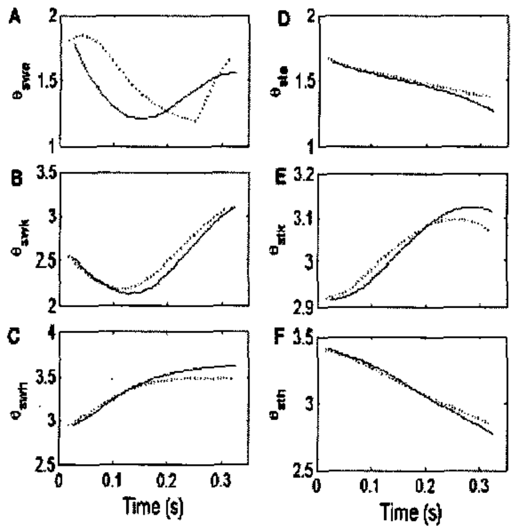

Figure 6. Simulation joint angles (solid lines) are compared with joint angles from biological gait data (dotted line). A) Swing ankle. B) Swing knee. C) Swing hip. D) Stance ankle. E) Stance knee. F) Stance hip.

When comparing the local gradient based and genetic algorithm type search used by the final optimizer for the same initial plant state and the same initial optimizer guess we observed either the results of the two methods to be almost identical with no apparent gain in using the slower genetic algorithm search or the optimization results of the two methods were very different and at successive time increments the genetic algorithm based approach began to give increasingly poor results.

IV. Discussion

From biological gait data we observed all joints collected behavior in terms of angular momentum distribution. The collected behavior, i.e. angular momentum primitives and their respective gait dependent normalized distributions are invariant with speed. We also observed that using these angular momentum primitives reduces the dimensionality of the problem; for sagittal plane rotation we find three primitives that effectively explain all biological walking data. Based on these observations we proposed a novel control architecture.

Our current control architecture utilizes two distinct optimizers, the initial optimizer and the final optimizer. The advantage of having the initial optimizer is that it quickly generates highly biomimetic results even though no predefined joint trajectories are employed. Using the speed invariant angular momentum primitives effectively reduces the search in the large N dimensional space to N one-dimensional optimization problems. The optimization of N DOF using D search points per DOF requires D^N computations. By our method, this optimization has been reduced to $D \cdot N$ computations. Even with this reduction in the number of computations, an initial guess that is very close to the global minimum of the entire N-dimensional space can still be found. Having an initial guess in the vicinity of the optimal solution simplifies the final optimizer's search. The final optimizer's search can then be only medium-local and fast enough so that real time control is achievable.

For the sagittal eight DOF model with known dynamics and no external disturbances, the initial optimizer gave notably biomimetic results. For this simulation the presence of the final optimizer has not offered a particular advantage to our control scheme; the visual solution of the figure walking was not different from the solution found using the final optimizer. However, for the control of a physical robot, i.e., a plant embedded in realistic conditions, we anticipate an important role for the final optimizer. The initial optimizer, using the current architecture, is most likely insufficient to reject various disturbances to the plant, so that the initial optimizer's solution will need to be improved by the final optimizer.

To further improve our control methodology we are currently experimenting with variations in the input spin PC distributions. We are varying only the first three PCs about the initially estimated value, obtained by the method described earlier. For each slightly varied combination of the first three PC's we repeat the same procedure, as with the original initial optimizer, of solving N one-dimensional problems and then to obtain the joint cost function for the whole plant. Finally, among all probed combination of the first three PC distributions we choose the one with minimal cost. As our preliminary results suggest, this procedure eliminates errors in the initial estimation of the spin distribution and it also rejects the numerical error more robustly. We hope that in this way we might address significant disturbances on the plant. With this improvement of our initial optimizer, our hope is to completely eliminate the final optimizer from the control loop.

For very large disturbances we anticipate a switching mechanism that will completely end the walking task and concentrate on pure balancing mechanisms. For the control of a physical robot, we anticipate having an adaptive control scheme. Also, as indicated in Fig. 4, we plan to experiment with cost function updating mechanisms that we hope will improve the quality of motion in a biomimetic and stability sense. In this way our controller will not just address the real dynamical response of the robot not anticipated with a physical model, but it will also adapt for specific dynamical posture cases when some of the cost function terms would need to dominate over others.

In this study, the two dimensional 8 DOF sagittal model served as the most simplified test bed (or a toy model) for the presented control methodology. Our ultimate goal is real time control of a morphologically realistic humanoid robot. In future investigations, we feel exploiting invariant angular momentum primitives in control may prove critical to achieving biological realism in legged robots, orthoses and prostheses.

Acknowledgment

The authors thank Paolo Bonato and Jennifer Lelas at the Spaulding Rehabilitation Hospital Gait Laboratory, Boston, Massachusetts for their helpful suggestions and support.

REFERENCES

[1] J. Slotine and W. Li, "Applied Nonlinear Control", Prentice Hall, New Jersey 1990.

[2] S. Schaal, "Is imitation learning the route to humanoid robots?," *Trends in Cognitive Sciences,* vol. 3, pp. 233-242, 1999.

[3] M. H. Raibert, "Legged Robots that Balance", Cambridge, MA, MIT Press, 1986.

[4] R. A. Brooks, C. Breazeal, M. Marjanovic, B. Scassellati and M. Williamson, The Cog Project: Building a Humanoid Robot, *Lecture Notes in Computer Science*: Springer, 1999.

[5] K. Hirai, "Current and future perspective of Honda humanoid robot," *Proceedings of the 1997 IEEE/RSJ International Conference on Intelligent Robot and Systems,* Grenoble, France:IEEE, New York, NY, USA. pp. 500-508, 1998.

[6] K. Hirai, M. Hirose, Y. Haikawa and T. Takenaka, "The development of Honda humanoid robot," *IEEE International Conference on Robotics and Automation,* Leuven, Belgium:IEEE, New York, NY, USA. pp. 1321-1326, 1998.

[7] G. Pratt, "Legged Robots: What's New Since Raibert," *IEEE Robotics and Automation Magazine. Research Perspectives*, pp. 15-19, 1999.

[8] M. Popovic, A. Goswami and H. Herr, "Review of CP/ZMP, FRI and ZSCP," (unpublished) to be submitted to International Journal of Robotics Research, 2004.

[9] A. Goswami, "Postural stability of biped robots and the foot rotation indicator (FRI) point", International Journal of Robotics Research, July 1999.

[10] F. C. Anderson, and M.G. Pandy, "Dynamic optimization of human walking", Journal of Biomechanical Engineering, vol. 123, October 2001.

[11] M. Popovic, A. Hofmann and H. Herr, "Angular Momentum Regulation during human walking: Biomechanics and Control," Proc. of the 2004 IEEE International Conference on Robotics and Automation (ICRA 2004), pp. 2405-2411, 2004.

[12] S. Kajita, O. Matsumoto, and M. Saigo, "Real-time 3D walking pattern generation for a biped robot with telescopic legs," Proc. of the 2001 IEEE International Conference on Robotics and Automation, pp. 2299-2306, 2001.

[13] S. Kajita and A. Kobayashi, "Dynamic Walk Control of a Biped Robot with Potential Energy Conserving Orbit," Trans. SICE 23-3, pp. 281-287, 1987.

[14] S. Kudoh, and T. Komura, "C2 Continuous Gait Pattern Generation for Biped Robots", IROS 2003.

[15] S. Kajita, F. Kanehiro, K. Kaneko, K. Fujiwara, K. Harada, K. Yokoi, H. Hirukawa, "Resolved Momentum Control: Humanoid Motion Planning based on the Linear and Angular Momentum", IROS 2003.

[16] Simon F. Giszter, Ferdinando A. Mussa-Ivaldi, and Emilio Bizzi, "Convergent force fields organized in the frog's spinal cord," Journal of NeuroScience, 13(2):467-491, 1993.

[17] K. A. Thoroughman and R. Shadmehr, "Learning of action through adaptive combination of motor primitives," Nature, 407:742-747, 2000.

[18] S. Schaal and C. G. Atkeson, "Constructive incremental learning from only local information," Neural Computation 10,8:2047-2084, 1998.

[19] T. D. Sanger, "Human arm movements described by a low-dimensional superposition of principal component," Journal of NeuroScience, 20(3):1066-1072, 2000.

[20] A. Fod, M. J. Mataric and O. C. Jenkins, "Automated Derivation of Primitives for Movements Classification," Autonomous Robots, 12(1):39-54, 2002.

[21] M. Popovic, W. Gu, and H. Herr, "Conservation of Angular Momentum in Human Movement," in *MIT AI Laboratory-Research Abstracts, 2002*, (2002), pp. 231-232.

[22] H. Herr, G. P. Whiteley, D. Childress, "Cyborg Technology–Biomimetic Orthotic and Prosthetic Technology," *Biologically Inspired Intelligent Robots*, Bar-Cohen, Y. and C. Breazeal, Eds., SPIE Press, Bellingham, Washington, 2003, pp. 103-143.

[23] W. Gu, "The Regulation of Angular Momentum During Human Walking", Undergraduate Thesis, Physics Department, MIT, June 2003.

[24] M. Popovic and H. Herr, "Angular Momentum Regulation during Human Walking," (unpublished) submitted to *Journal of Experimental Biology*, 2004.

[25] Tilley, A. R., and Dreyfuss, H. (1993) "The measure of man and woman," *Whitney Library of Design*, an imprint of Watson-Guptill Publications, New York.

[26] Winters, D. A. (1990) "*Biomechanics and Motor Control of Human Movement*," John Wiley & Sons, Inc., New York.